HAL
open science

Simulation of Low Nickel Content Alloys For Industrial Ground Fault Circuit-Breaker Relays

Oualid Messal, Fabien Sixdenier, Laurent Morel, Noël Burais, Thierry Waeckerle

To cite this version:

Oualid Messal, Fabien Sixdenier, Laurent Morel, Noël Burais, Thierry Waeckerle. Simulation of Low Nickel Content Alloys For Industrial Ground Fault Circuit-Breaker Relays. IEEE Transactions on Magnetics, 2014, 51 (6), pp.6991580. 10.1109/TMAG.2014.2384004 . hal-01374152

HAL Id: hal-01374152

https://hal.science/hal-01374152v1

Submitted on 29 Sep 2016

HAL is a multi-disciplinary open access archive for the deposit and dissemination of scientific research documents, whether they are published or not. The documents may come from teaching and research institutions in France or abroad, or from public or private research centers.

L'archive ouverte pluridisciplinaire **HAL**, est destinée au dépôt et à la diffusion de documents scientifiques de niveau recherche, publiés ou non, émanant des établissements d'enseignement et de recherche français ou étrangers, des laboratoires publics ou privés.

Simulation of Low Nickel Content Alloys For Industrial Ground Fault Circuit-Breaker Relays

Oualid Messal[1], Fabien Sixdenier[1], Laurent Morel[1], Noël Burais[1] and Thierry Waeckerlé[2]
[1]Université de Lyon, Université Lyon 1, CNRS UMR 5005 AMPERE,
43, Bld du 11 Novembre 1918, Villeurbanne, F69622, France
[2]Aperam Research Center, Imphy, F58160, France

***Abstract*— The aim of this paper is to simulate the performances of a ground fault circuit-breaker (GFCB) relay with new low nickel content alloys. Indeed, in the construction industry, the materials become more expensive as their nickel content increases. Moreover, the demand for nickel is particularly sensitive to the economic conjuncture. Therefore, an original electromagnetic relay model has been developed and validated in different working conditions (current amplitude, frequency, temperature). A dedicated magnetic characterization of materials is needed, using basically a usual and industrial GFCB relay for reference and design data in modeling. First, the magnetic model of the relay is built and checked against experimental data. The simulation may predict the tripping current threshold of the relay. On the other hand, new low nickel content alloys for relay parts are studied in this framework, thanks to the developed model. The effect of temperature on the magnetic properties of the candidate materials and the electrical performances of the virtual relays is presented. The results, analysis, and conclusions are given. Finally, a first attempt to predict the economic gain made with a change of material is made.**

***Index Terms*— AC circuit- breaker, Dynamic hysteresis, Eddy currents, FeNiCr alloys, Optimization, Temperature.**

I. Introduction

The protection of persons and domestic or professional appliances against electric shocks must be ensured in conformity with standards. The IEC60479 standard [1] introduces the effects of the AC current of a frequency 50 Hz on human beings and livestock. In particular, the threshold of ventricular fibrillation increases with frequency (*f*). One can see in Fig. 1, that the tripping factor (tripping current at the frequency *f* over the tripping current at the rated frequency of 50 Hz) increases versus frequency according to an exponential curve. The waveform of the current for the given frequencies is sinusoidal. In this respect, manufacturers have developed ground fault circuit-breakers (GFCB) that are compatible with this threshold (limit curve) and its frequency variation. They ensure that the thresholds of the protection devices remain below the ventricular fibrillation curve defined in the standard IEC60479 for each frequency.

A GFCB [2] usually falls into three parts: the differential current sensor, the electronic circuit, and the highly sensitive electromagnetic relay, the latter being the framework of this paper. In order to be effective, the relay parts require both high magnetic force (i.e., high magnetic saturation J_S) and low energy consumption (i.e., high dynamic relative permeability μ_r, low coercive field H_c) to trip the breaker under the effect of small electrical fault (a few tenth of mA). The Fe–48%Ni alloy (Supra50) meets these requirements, providing J_s = 1.6 T, $\mu_r \approx 120000$ and $3 < H_c < 4$ A/m after a specific heat treatment. Its temperature stability is very good as the Curie point (T_c) is around 450 °C, far from room temperature (RT). Due to the massive magnetic circuit (1 mm depth), a lot of eddy currents can occur in the magnetic circuit in dynamic regimes. These eddy currents reduce the F_{coil} force (see section II). This means that the needed current amplitude has to increase in order to have a sufficient force to make the relay trip. If engineers want to build a model to predict a correct behavior of the relay, eddy currents that can occur in the magnetic circuit have to be taken into account.

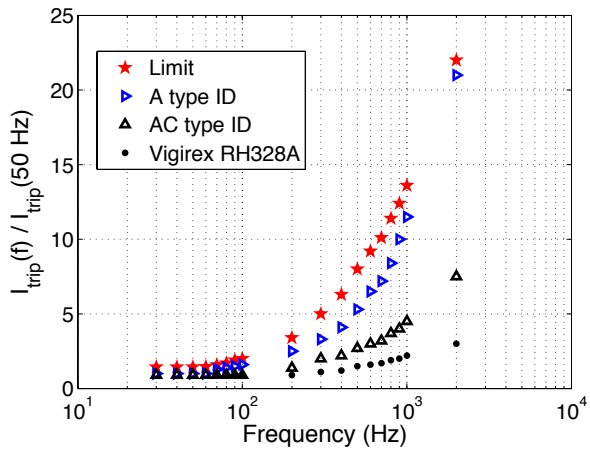

Fig. 1. Variation of the ventricular fibrillation threshold (as per IEC 60479-2) and thresholds of various RCDs set on 30 mA, as a function of frequency (the figure is plotted from data given in [2]).

Moreover, engineers would like to virtually test the relay's potential behavior with a magnetic circuit made of another material. This last material should realize a compromise between an affordable economic price and good performances. Besides its usual Supra50 (Fe–48%Ni) grades, Aperam [3] develop several FeNiCrCu [4], [5] near 30%Ni (wt) and Invar alloys (36%Ni), as a new material family providing both reduced nickel content, reduced remanent induction B_r, higher dynamics (with an electrical resistivity $80 < \rho_{el} < 100\ \mu\Omega$.cm) keeping good DC magnetic properties ($H_c \approx 3 - 10$ A/m,

Corresponding author: O. Messal (oualid.messal@univ-lyon1.fr).
Digital Object Identifier inserted by IEEE

$\mu_r \approx 20000$). However, these alloys present two main drawbacks toward this application: their J_s is lower than the Supra50's one (e.g., lower magnetic force) and they do not ensure the same temperature stability (their T_c is lower) at the operating temperatures of the relay [-25, 85 °C]. Thus, changes in their characteristics must be anticipated.

This work deals with the study of the ability of these new low nickel FeNi alloys, designed as a potentially less expensive solution compared to the Supra50. Based on [6], the original approach has been extended to take into account temperature, well adapted to the dynamical behavior description of high sensitivity electromagnetic relay.

In the next sections, we have first carried out an analytical study of the relay in order to analyze qualitatively its operation. This study is based on very simplistic assumptions. However, it helps us to evaluate the nature of the encountered phenomena and clarify our needs in terms of data. It is limited to the linear regime. In the next step, a short recall of the modeling approach of the relay and the dynamic behavior of the material is made. Then, once the model is established, the modeling approach is validated against experimental measurements. The relay model is subsequently used to simulate what would be its behavior with other magnetic alloys at room temperature (RT) and at 85 °C. Finally, a first attempt to predict the economic gain made with a change of magnetic materials is made.

II. Operating Principle of The High-Sensitivity Electromagnetic Relay

The relay magnetic circuit (Fig. 2) is composed of an armature (or core), a permanent magnet, and a mobile part in rotation around one of the core leg end where a spring is attached in order to facilitate such movement. The magnet's force F_{Magnet} is used here to counterbalance the force F_{Spring} of the spring, such as the mobile part closes the magnetic circuit when there is no electrical defect (situation $F_{Magnet} > F_{Spring}$). The appearance of a leakage current induces an e.m.f. across the terminals of the secondary coil, which supplies the relay. During a favorable current half-period, the flux generated in the magnetic circuit formed by the closed relay is of opposite sign to the flux produced by the magnet: then a new force F_{coil} is added to the spring's one and results in the relay opening (situation $F_{coil} + F_{Spring} > F_{Magnet}$). The operating principle is illustrated in Fig. 2 below.

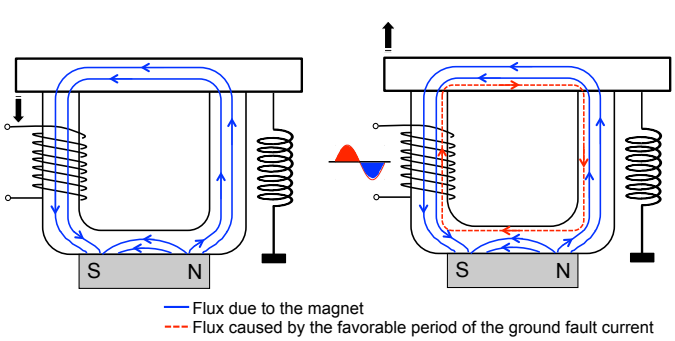

Fig. 2. Operating principle of the relay.

A. Simplified Analytical Approach of the Frequency Behavior of the Relay Tripping Current

The magnet biases the relay magnetic circuit (mean length, L) to a magnetic polarization level J_p, causing the magnet force $F_{Magnet} = J_p^2.S/2\mu_0$). The design and the air gaps are performed in such a way that the magnet polarization J_p is high to create a high enough magnetic force for a magnetic circuit section as small as possible (FeNi cost). But, J_p should not be too high to avoid saturating the material because we also need a high differential permeability μ_{rdiff} around the polarization point J_p (see below). In practice, J_p is of the order of 0.8 T.

When there is no electrical defect, $F_{Magnet} > F_{Spring}$ (equilibrium position). Indeed, in practice, each produced relay is set according to a precise amount $\Delta F = F_{Magnet} - F_{Spring}$. The imbalance is introduced by a 3rd force F_{coil} coming from the relay coil (number of turns N, field H_{coil}), fed by the current I stemming from the electrical fault detection torus. Once $F_{coil} = \Delta F$, the balance is broken and at this moment, the current I in the coil is the minimum tripping current I_{trip} of the relay.

Let us recall that if e denotes the thickness of the relay material, the skin effect is considered negligible when $\delta \geq e/2$. If we call ΔJ the variation of the polarization in the magnetic circuit under the effect of the bias field of the magnet H_p around $J_p(H_p)$, we have in a very crude model:

If $\delta < e/2$:

$$B \approx J = (2\delta / e) \cdot \Delta J(J_p) \tag{1}$$

If $\delta \geq e/2$:

$$B \approx J = \Delta J \tag{2}$$

In practice, the skin effect is not negligible, so, we focus on this case. Considering $\Delta J(H_{coil})$ quasi-linear around a polarization point of the magnet (Fig. 3 of the Supra50 alloy):

$$\Delta J\left(J_p\right) = \mu_0 \mu_{rdiff} H_{coil} \tag{3}$$

We deduce that:

$$B \approx \frac{2\delta}{e} \mu_0 \mu_{rdiff} H_{coil} \approx \frac{2}{e}\sqrt{\frac{2\rho}{\mu\omega}} \mu_0 \mu_{rdiff} H_{coil} \tag{4}$$

And according to the Ampere's theorem:

$$H_{coil} = \frac{N I_{trip}}{L} \tag{5}$$

The expression of B becomes:

$$B = \frac{2N\sqrt{\mu_0}}{\sqrt{\pi} e L} \sqrt{\rho \mu_{rdiff}} \frac{i_{trip}}{\sqrt{f}} \tag{6}$$

The relay tripping occurs when:

$$\Delta F = Cte = F_{coil} = \frac{B^2 S}{2\mu_0} \tag{7}$$

Whence

$$B = \sqrt{\frac{2\mu_0 \Delta F}{S}} = \frac{2N\sqrt{\mu_0}}{\sqrt{\pi} eL}\sqrt{\rho\mu_{rdiff}}\frac{I_{trip}}{\sqrt{f}} \tag{8}$$

Thus:

$$I_{trip} = \frac{\sqrt{\pi} eL}{2N\sqrt{\mu_0}\sqrt{\rho\mu_{rdiff}}}\sqrt{\frac{2\mu_0 \Delta F}{S}}\sqrt{f} \tag{9}$$

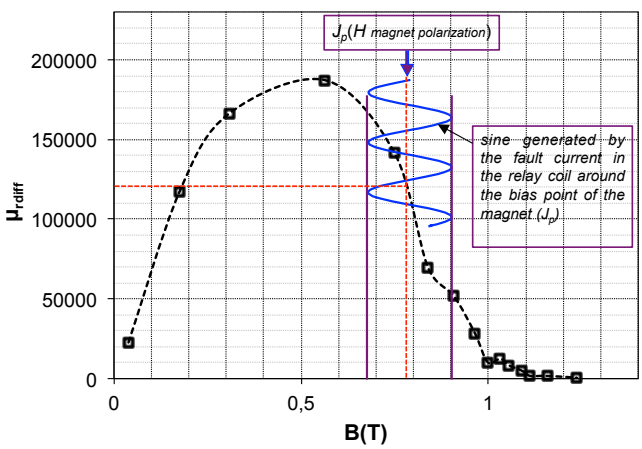

Fig. 3. Differential permeability of the soft magnetic material constituting the relay (the Supra50 alloy)

We deduce that the relay tripping current is independent of frequency when $\delta \geq e/2$ (when the skin effect is negligible) and it is given as a function of $\sqrt{f}$ when $\delta < e/2$.

The expression of the tripping current in Eq. (9) reproduces qualitatively the same frequency behavior as in Fig. 1. This relationship is sufficiently interesting to evaluate the influence of each characteristic (e, N, ρ, μ_{rdiff}, S, ΔF) on the tripping current; however, it does not enable an accurate prevision of the relay dynamic behavior. Indeed, this study is based on very simplistic assumptions (constant section of the magnetic circuit of the relay, witch is not the case in industrial GFCB, $\Delta J(H_{coil})$ linear…). Besides, we have no data concerning the ΔF term. It is not always either well defined or well quantified.

III. Relay and Material Modeling Protocol

A. Relay Geometry and Magnetic Equivalent Circuit

Fig. 4 shows a photograph of the investigated relay and Fig. 5 shows the scheme of the geometry and the adopted magnetic circuit topology. The device would be modeled by flux tubes instead of finite elements (FE) given the complexity of the problem, the number of unknowns (section II-C), the long computation time with FE, and the necessity of accurate dynamical description taking into account eddy currents.

Fig. 4 shows three kinds of flux tubes: air-gap flux tubes, a magnet flux tube and other magnetic flux tubes accurately representing the dynamic behavior of the soft magnetic relay parts. The geometric flux tubes parameters are their

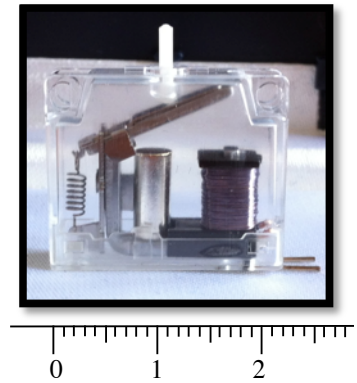

Fig. 4. The investigated GFCB relay produced and marketed by Schneider Electric [7] (the unit of the ruler is in cm).

dimensions (length, section, depth) and parameters that can describe the magnetic behavior of each flux tube. Each flux tube constitutes a "magnetic circuit component" that must be linked to other magnetic or electrical circuit components. This association fulfills the nodes law and the Ampère's theorem obtained by analogy between magnetic and electric circuits [6]. The coupling variables are $d\phi/dt$ and $H.l$ (where ϕ = magnetic flux, H = excitation field on the surface of the flux tube, l = mean length of the tube, $H_j.l_j = N_k.i_k$ = k-th MMF source).

The tools used for simulation are Matlab and Simulink with the SimPowerSystems Blockset toolbox.

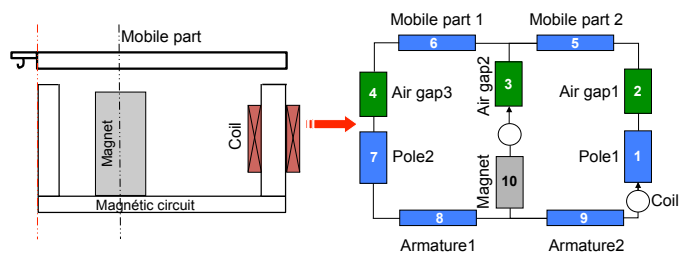

Fig. 5. Scheme of the geometry of the relay (left) and its MEC (right).

The magnet properties (B_r, μ_r) are the essential data, which define the relay tripping conditions. Besides, the major criteria are the dimensions of the air gaps and the number of turns. The leakage flux is supposedly negligible when the mobile part closes the circuit (which is the case for our study).

B. Soft Magnetic Material Modeling

In each soft ferromagnetic part (armature, pole, and mobile part) a dynamic model that takes into account the eddy currents that can occur in the magnetic circuit is implemented. The dynamic model is called the "Diffusion and Wall Motion" (DWM) model. The main assumptions of the model are:

- the study domain is a rectangular sheet where edge effects are neglected.
- the magnetic field is supposed to be unidirectional (along the length of the sheet).
- the material is isotropic and its electrical conductivity σ_{el} is homogeneous.

It takes into account the skin effect developed in the material and it comes from the magnetic field diffusion

equation reduced to a 1D formulation.

Due to the symmetry of the system, this equation is solved by using the Finite Difference (FD) method on the half-thickness (d/2) of the sheet cross section. The FD system formulation leads to a nonlinear algebraic system that has to be solved. This system contains as many equations as the number of spatial discretization nodes of the studied domain. This model uses a static law $H_{stat}(B)$ or $B(H_{stat})$. Neglecting static hysteresis, we have considered the an-hysteretic curve determined from a measured major quasi-static loop at 0.1 Hz. The DWM model is accurate at high frequencies (see Fig. 6). The dynamic model parameters are identified from measurements performed at 2 kHz using the simplex method [10]. The parameter values are then used to simulate the dynamic behavior at different frequencies below 2 kHz with very good accuracy (for example, see the simulation at 300 Hz in Fig.6-b). More details of this model can be found in [9].

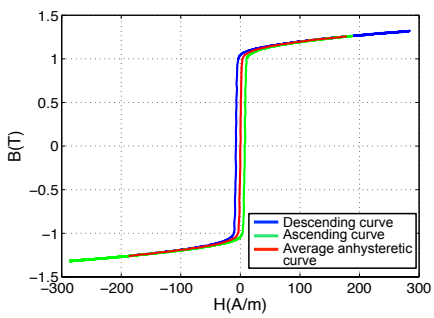

a) An-hysteretic curve used in dynamic modeling just below.

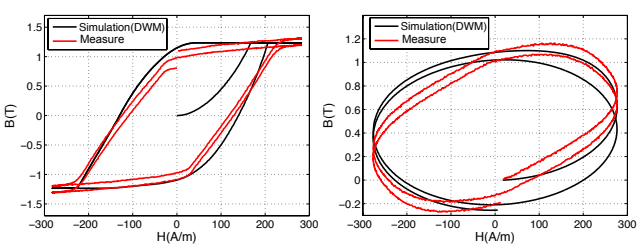

b) Dynamic hysteresis loops in the Supra50 alloy at RT at f = 300 Hz (left) and f = 2 kHz (right).

Fig. 6. Dynamic behavior modeling of the Supra50 alloy.

C. Experimental Measurements and Relay Model Validation

In order to validate the developed relay model, experiments have been performed on the demonstrator device for different frequencies under sine current excitation. The residual current device for which tripping is ensured, according to the IEC 6100812 international standard [11], allows the application of slowly rising intended currents, as shown in Fig. 7 (blue curve). The relay is fed with a sine current source until tripping. The excitation coil is supplied with a programmable excitation current (different frequencies). The waveforms of the current (i(t)) and the voltage of the relay coil (u(t)) are recorded on an acquisition board. When the tripping relay occurs, the flux in the air gaps falls suddenly and a transitional phase is sharply marked and the phase shift between u(t) and i(t) becomes very low (see Fig. 7). The ratio u_{max}/i_{max} of the period just before the tripping is used to define Z_{trip} (even if

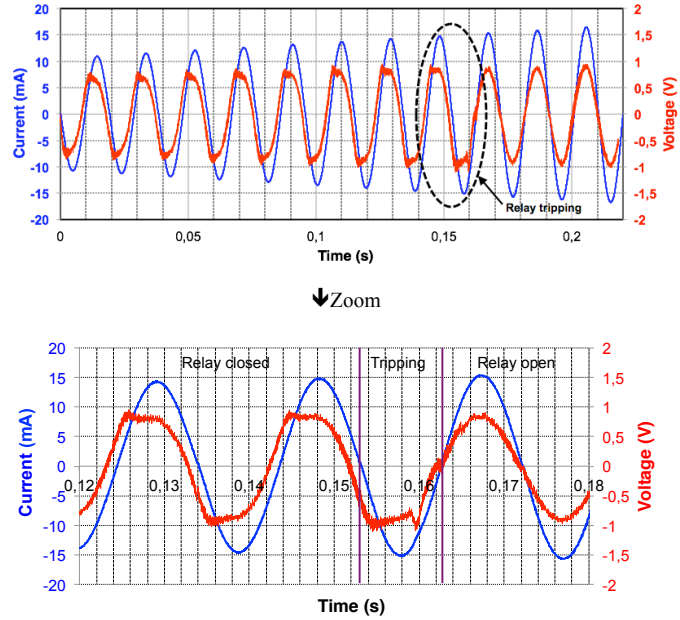

Fig. 7. Measured current and voltage waveforms at 50 Hz with a slowly rising current and zoom on the tripping conditions at room temperature.

the voltage waveform is not sinusoidal), for each frequency.

In order to correctly simulate the electromagnetic relay, some unknowns have to be determined with the help of the experiments. The magnet properties (B_r, μ_r), the number of turns of the coil, and the three air-gaps lengths are optimized using the simplex method. The objective function to minimize is the quadratic error between the simulated and measured Ztrip. Values of the parameters that minimizes the objective function are reported in Table I.

TABLE I
OPTIMIZED PARAMETERS

Number of turns	Air-gap1 (μm)	Air-gap2 (μm)	Air-gap3 (μm)	B_r (T)	μ_r
508	15.52	0.108	15.52	0.72	3.9

With the values mentioned in Table I, the measured and simulated Z_{trip} curves versus frequency at RT are shown in Fig. 8.

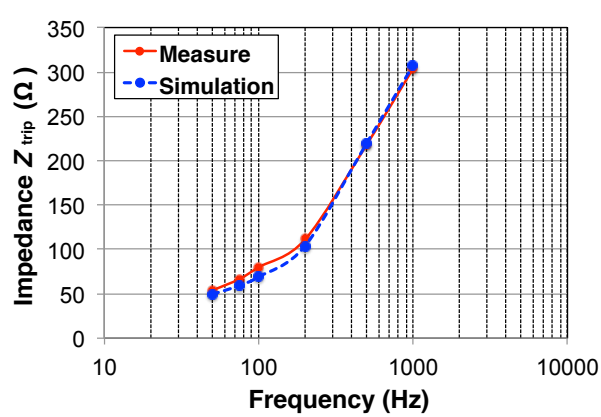

Fig. 8. Impedance vs frequency at room temperature

As it can be seen in Fig. 8, the measured and simulated Z_{trip} are in good agreement. This model will now be used to simulate virtual relays with a magnetic circuit made with different alloys than the Supra50.

IV. New Low Nickel Content Invar-Type Fe-Ni-Cr-Cu Alloys: Brief Presentation

In the construction industry, the higher nickel content of alloys makes them more expensive. In this regard, it should be noted that the demand for nickel is particularly sensitive to the economic conjuncture (see Fig.9).

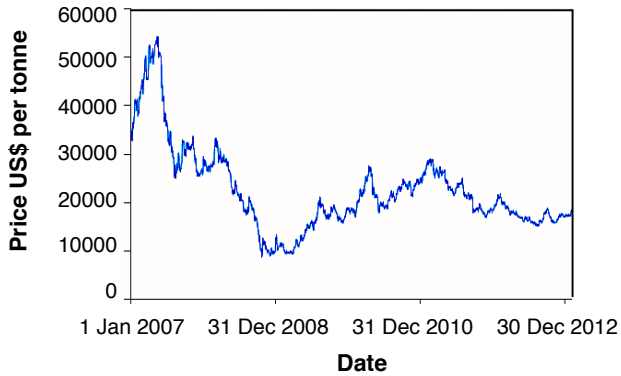

Fig. 9. Five-year nickel price graph (source: London Metal Exchange).

The nickel price graph over the last 5 years, extracted from the London Metal Exchange [13], is given in Fig. 9. One can see that the nickel price peaked at more than 50 k$/tonne in March 2007 and subsequently declined to 10 k$/tonne in February 2009. In that way, recently, soft magnetic Invar type Fe-Ni-Cr-Cu alloys (H_c=2.5 to 12 A/m), exhibiting a stable and single phase fcc structure at ambient temperature, low T_c (100–250 °C), medium J_s (0.4 to 1.2 T) have been designed by Aperam Research Center in Imphy between 27 and 32%wt-Ni. Many quaternary Fe-Ni-Cr-Cu compositions have been studied in [4] in the range 28–36%Ni, 0–13%Cu, 0-3%Cr in order to determine the γ phase stability and the magnetic properties. Associating copper and chromium alloying in such Invar-type low nickel fcc soft magnetic materials allows J_s and T_c (Fig. 10) to be significantly increased, with a moderate deterioration of soft magnetic properties.

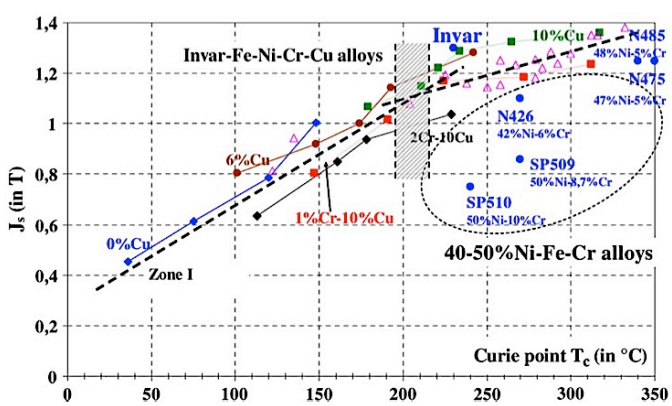

Fig. 10. Saturation polarization versus Curie point for a wide set of FeNiCr. (≥ Fe50%Ni) and Invar-type FeNiCrCu alloys (extracted from [4]).

In the next section, the Supra50 relay model developed before is used to simulate the relay made of some of these new low nickel content Invar type Fe-Ni-Cr-Cu alloys at room temperature (RT) and at the maximum working temperature 85°C.

V. New Low Nickel Content Alloys for a Relay Device?

A. Extension of the DWM Model to Take into Account the Temperature

Five low nickel content FeNi(Cr,Cu) alloys, provided by Aperam Research Center in Imphy are selected in order to study their ability to replace the Supra50 alloy in the relays (see Table II). Almost all the selected alloys (except TD522-5) are situated within the gray zone of Fig. 10. The Supra50 (Fe48/Ni) is located at the top right of the same figure.

TABLE II
Low Nickel Alloys Selection for The Relay Simulation

Alloy	Composition	J_s (T)	T_c (°C)
Supra36	Fe-36%Ni	1.3	250
SV315	F-31%Ni-2%Cr-6%Cu-0,2%Mn	1.00	190
TD522-5	Fe-30,5%Ni-2%Cr-6,4%Cu-0,2%Mn	0.953	157
SV285	Fe-30%Ni-6%Cu-0,3%Mn	1.085	205
TD565-4	Fe-30%Ni-1%Cr-10%Cu-0,2%Mn	0.975	191

Quasi-static and dynamic hysteresis loop measurements were made, first at room temperature and then at 85 °C on ring samples. At each test temperature, the an-hysteretic curve is determined from a quasi-static hysteresis loop measured at 0.1 Hz for each of the investigated alloys. In addition, a double four-point probe measurement method is used to determine the electrical resistivity of ring specimens at high temperatures (namely at 85 °C) as well as at room temperature (RT) (see Table III). A detailed description of the method is reported in [12]. The measured dynamic loops at high frequencies, as mentioned previously, are used to identify the parameters of the DWM model. All these data are necessary for the DWM model. One can see, for example, in Fig. 11 the measured an-hysteretic curves at two temperatures and the electrical resistivity ρ_{el} versus temperature for the TD565-4 material.

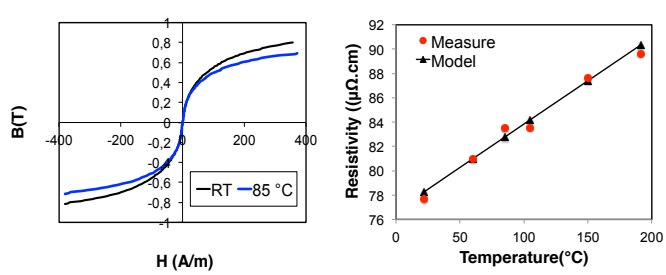

Fig. 11. An-hysteretic curves at two temperatures (left) and resistivity versus temperature (right) for the TD565-4 candidate material.

Once all the DWM parameters are known for each temperature, the DWM model is able to predict the dynamic

behavior at different temperatures. As an example, Fig. 12 illustrates the measured and simulated loops for the TD565-4 candidate material for f = 200 Hz and f = 2 kHz at RT and at 85 °C. One can see that the magnetic behavior has changed. The saturation induction is a bit lower and the loop is thinner at 85 °C than at RT. In each case, the DWM model is in good agreement with the measurements.

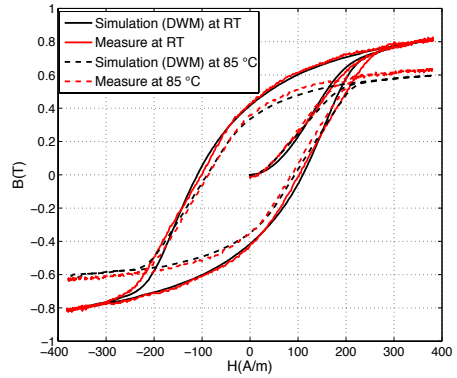

a) f=200 Hz

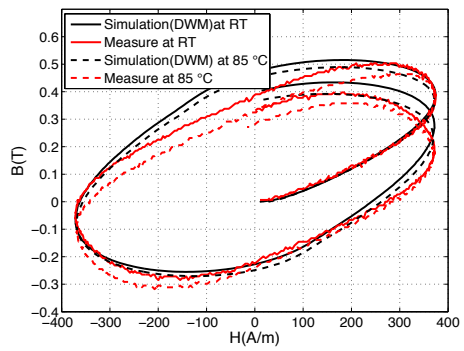

b) f=2kHz

Fig. 12. Measured and simulated loops for the TD565-4 candidate material at f=200 Hz at RT and at 85 °C.

B. Tripping Criterion

In order to predict the overall behavior of the electromagnetic relay built with the candidate materials, a tripping criterion is defined. When a candidate material is introduced in the model, the magnetic permeability of the material is not the same as the Supra50's one. This will change the reluctance of the magnetic circuit, the electrical impedance, and consequently the relay tripping current value. To study the tripping current, let us begin with a simplified scheme displaying the different forces acting on the mobile part of the relay (see Fig. 13).

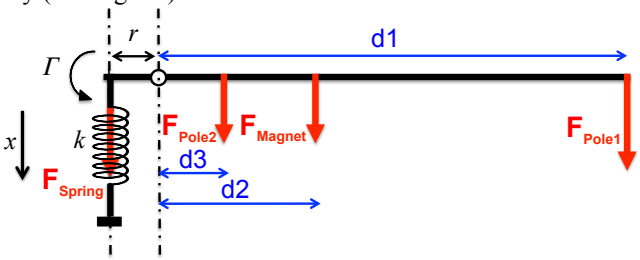

Fig. 13. Forces acting on the mobile part of the relay.

The relay tripping occurs when the magnetic torque, Γ_{mag} acting on the mobile part is lower than the spring torque. However, the value of the spring torque is unknown. Avoiding a direct difficult measurement of its stiffness, we chose another method to predict the tripping current without the knowledge of the torque spring magnitude. Starting from the tripping current data measured at various frequencies in the demonstrator relay (made of Supra50), the corresponding magnetic torque exerted on the moving part may be calculated at each tripping current value in the whole frequency range. This torque will be called "the reference magnetic torque in tripping conditions."

In the next step of calculation applied on a candidate alloy, at each test frequency, we determine the current value which allows the same torque as the Supra50 relay solution does, under the same dynamical solicitation (see Fig. 14).

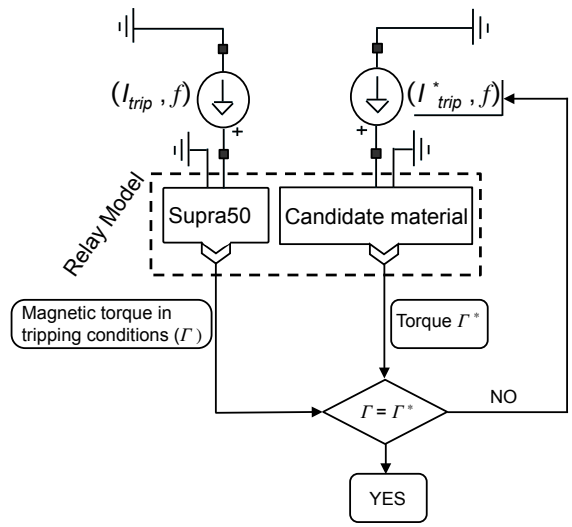

Fig. 14. Method to determine the tripping current for candidate alloys.

As an example, Fig. 15 shows the 50 and 500 Hz typical magnetic torque curves of the Supra50 relay in tripping conditions at room temperature and the simulated torque curves for the virtual new alloy relays. There is rather good agreement between all the torque curves. The excitation current levels necessary to obtain identical values as the reference magnetic torque in tripping conditions reflect the tripping of the virtual relays constructed from each candidate alloy. Thus, we determine the tripping current of a candidate material relay. The tripping factors I_{trip}/I_n as functions of frequency, for each of the investigated alloys, are superimposed in Fig. 15. As mentioned before, (9) gives such an assessment, but it remains essentially of a qualitative nature. However, the developed model accurately predicts this variation with the true elements of the relay.

It seems that there is a close connection between the differential permeability, μ_{rdiff} of the alloy and the tripping current value of the relay. Table III shows the maximum differential permeability μ_{rdiff_max} and the electrical resistivity ρ_{el} of the new low nickel content alloys in comparison with the usual Supra50. One can see that as μ_{rdiff_max} increases, the tripping current decreases. It should be emphasized that the analytical law in (9) confirms this analysis. It reveals a good inverse relationship between I_{trip} and μ_{rdiff}.

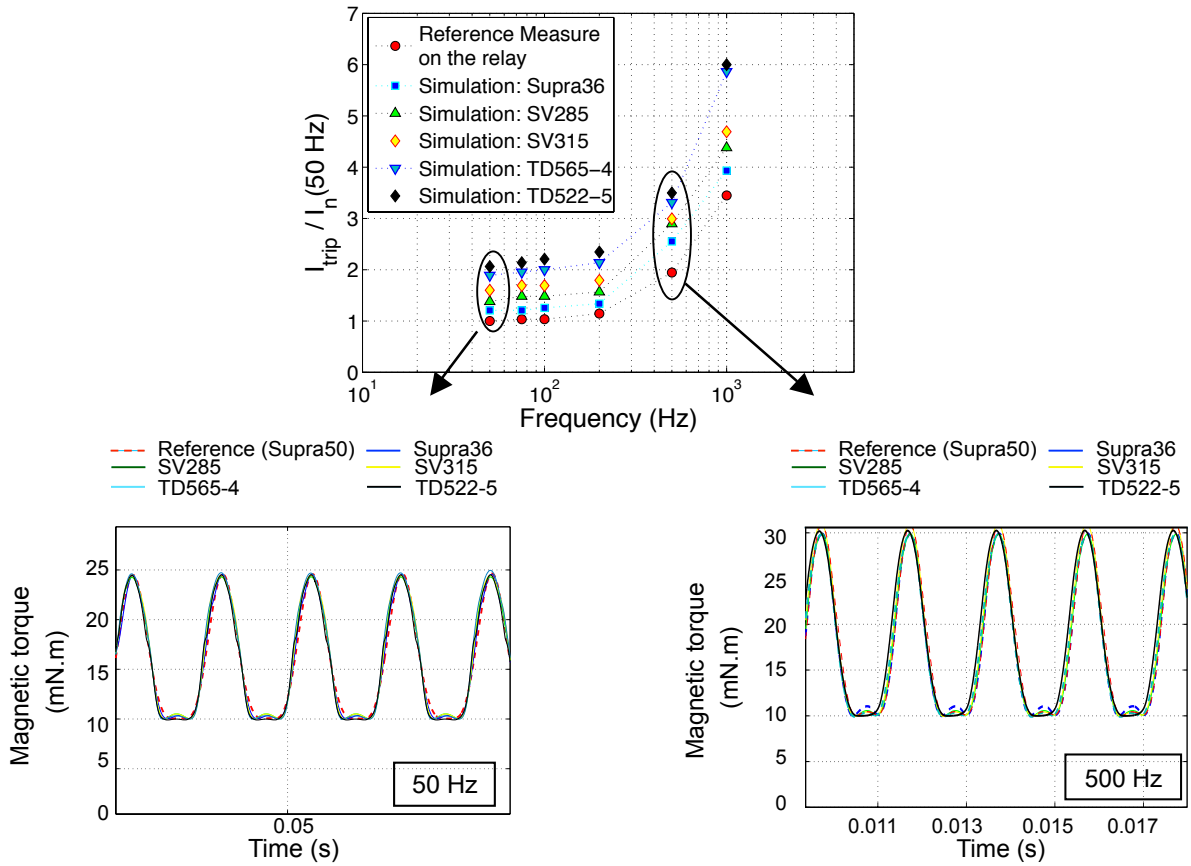

Fig. 15. Tripping factor I_{trip} /I_n vs frequency at RT (the nominal tripping current I_n is defined for the operating frequency (e.g., 50 Hz)).

TABLE III
LOW NICKEL CONTENT ALLOYS ' DIFFERENTIAL PERMEABILITY AND RESISTIVITY

Alloy	Composition	$\mu_{rdiffmax}$	ρ ($\mu\Omega$cm)
Supra50	Fe-48%Ni	190000	48
Supra36	Fe-36%Ni	76000	75
SV315	F-31%Ni-2%Cr-6%Cu-0,2%Mn	17000	87
TD522-5	Fe-30,5%Ni-2%Cr-6,4%Cu-0,2%Mn	14000	82.5
SV285	Fe-30%Ni-6%Cu-0,3%Mn	20000	80
TD565-4	Fe-30%Ni-1%Cr-10%Cu-0,2%Mn	15000	77.5

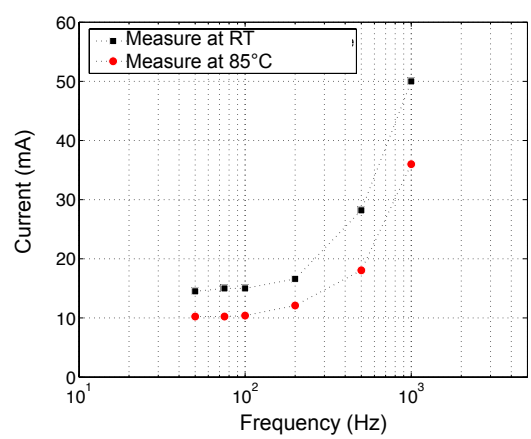

Fig. 16. Measured tripping current of the relay (of Supra50) as a function of frequency at 85 °C in comparison with the measured curve at RT.

C. *Effect of The Temperature on the Tripping Factor*

The development of these new materials for high-sensitivity relay devices requires a thorough knowledge of the application up to the limit working conditions. These requirements lead to conduct a thermal characterization of the relay at its maximum working temperature (85 °C). The tripping current at 85 °C has been measured with the same measurement process as at RT except that the relay was introduced in an oven. The results showed that the measured tripping current of the Supra50 relay at 85 °C is lower than the one measured at RT (see Fig. 16). This appears to be related to the increase of μ_{rdiff} of the constitutive alloy (Supra50) of the relay, but also to the increase of its electrical resistivity at 85 °C.

With exactly the same modeling process as reported above at RT (identification of dynamic models parameters, an-hysteretic curves, alloys conductivities), the current values at 85 °C are determined. The torque curves are calculated in the whole frequency range, fitting rather well again with the reference at 85 °C. The obtained tripping factor for all alloys is superimposed in Fig.17.

As expected, the current values are lower than those obtained at RT (i.e., the relay is more sensitive to differential faults). From the results presented in Fig. 15 and Fig. 17, it turns out that the Supra 36, SV285 and SV315 alloys have almost the same frequency behavior (with an offset) and the same temperature sensitivity as the Supra50 alloy. The variation ratio of the tripping current between RT and 85 °C for these materials is essentially the same as the Supra50's one, it is of the order of 1.44 to 1.48. For the other two alloys (TD565-4 and TD522-5), this is not the case. This ratio reaches, for example, 1.80 for the TD522-5 alloy. In view of these results, some of the new low nickel content alloys studied here (Supra36, SV285, and SV315) seem to be interesting possible replacements for the Supra50 alloy for the manufacture of relay parts. If engineers want to retrieve exactly the same tripping current (and not only the same frequency behavior) as the Supra50 relay, adjustments can be made on the relay (design parameters) or its environment. Indeed, the certification of new products requires different steps, especially when the safety of people is involved. This study was focused on the electromagnetic relay behavior used in a GFCB (The main role of GFCB is to protect people); thus, the redesign process can take two main directions with many sensitive parameters:

- redesign only the relay (increase cross section and/or number of turns, decrease the magnet polarization, decrease the stiffness of the spring,...).
- redesign the environment of the relay, the whole GFCB (the differential current sensor, the electronic circuit,...).

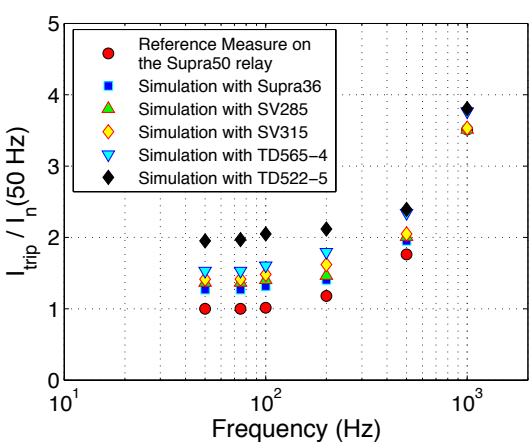

Fig. 17. Tripping factor I_{trip} /I_n vs frequency at 85 °C (the nominal tripping current I_n is defined for the operating frequency (e.g., 50 Hz)).

VI. Attempt of The First Economic Assessment

In this last section, we present a simple study allowing a first assessment of the economic contribution of the new low nickel content alloys studied in this work in comparison with the reference solution of Supra50. To do so, we assume a magnetic circuit of the same size as the Supra50's one. The question that arises is: what is the gain in mass of nickel in the magnetic circuit of the relay and then what would be the economic gain?

The accompanying table (Table IV) provides the Supra50's data and those of a candidate alloy, for example, the Supra36 alloy. These data are needed to estimate the added value from an economic point of view of these new low nickel content alloys in comparison to the usual Supra50.

TABLE IV
Comparison Between the Supra50 and A Candidate Alloy

	Supra50	Supra36
Composition	Fe–50%Ni	Fe–36%Ni
Density (g/cm^3)	8.2	8.1
Estimated volume of the magnetic circuit of the relay (mm^3)	222.16	222.16
Mass of the relay magnetic circuit (g)	1.82	1.79
Mass of Ni (per relay) (g)	0.91	0.644
Price of Ni (per relay) (in US cents)	0.91 to 4.91	0.644 to 3.48

These considerations clearly show that the mass of Ni gained with the new alloys compared to the existing commercial material (Supra50) can be estimated to 0.266 g per relay. Based on the following assumptions:

- a total of 10 millions relays sold every year,
- a nickel price fluctuating between 10 to 54 k$ per tonne (see Fig. 9),

Manufacturers of magnetic materials and related products can expect a yearly gain estimated between 26 to 143 k$.

VII. Conclusion And Prospects

The paper deals with the use of new alloys to realize electromagnetic relays for circuit breakers that may be used as a replacement to Supra50 magnetic alloy. We have elaborated a phenomenological model in order to predict the overall behavior of an electromagnetic relay based on the knowledge of its constitutive alloy (Supra50) and a fine description of its geometry. New low nickel content alloys are then investigated in this framework thanks to the developed model. We stated that the choice of new economic FeNi suitable for the manufacture of the relay parts is possible. Indeed, some materials seem to be interesting to replace the Supra50 alloy and have the opportunity to propose cheaper solutions for the manufacture of relay parts. They have almost the same frequency behavior and the same temperature sensitivity as the Supra50 alloy. Thanks to the developed model, it is possible to design new electromagnetic relays made with different magnetic circuits (with these low nickel content alloys). The main drawbacks of the new alloys can be compensated by design parameters of the relay (example: number of turns) or by changing its environment (example: the differential current sensor).

References

[1] IEC60479–2, "Effects of current on human beings and livestock, special aspects," *International standard*, 2007.

[2] R. Calvas, "Residual current devices in LV," *Schneider Electric technical publication*, 1999.
[3] http://www.aperam.com/alloys-imphy/.
[4] T. Waeckerlé, "Low nickel content FCC alloys: Recent evolution and applications," *IEEE Trans. on Mag*., vol. 46, no.2, pp. 326- 332, 2010.
[5] T. Waeckerlé, O. Danylova, "Austenitic iron-nickel-chromium-copper alloy," US patent 20100102910, 2010.
[6] F. Sixdenier & all, "Dynamical models for eddy current in electromagnetic cores introduced in an FE-tuned magnetic equivalent circuit of an electromagnetic relay," *IEEE Transacions on Magnetics*, vol. 44, no. 6, 2008.
[7] Schneider Electric, http://www.schneider-electric.com.
[8] Zhai Guofo, Wang Qiya, Ren Wanbin "An output space-mapping algorithm to optimize the dimensional parameter of electromagnetic relay," *IEEE Trans. Magn.,* vol. 47, no. 9, pp. 2194–2199, Sept. 2011.
[9] M. A. Raulet & all, "The magnetic field diffusion equation including dynamic hysteresis: A linear formulation of the problem," *IEEE Trans. Magn.,* vol. 40, no. 2, pp. 872–875, Mar. 2004.
[10] O. Messal, F. Sixdenier, L. Morel and N. Burais, "Temperature dependent extension of the Jiles– Atherton model: Study of the variation of microstructural hysteresis parameters," *IEEE Transactions on Magnetics,* vol. 48, no. 10, pp. 2567- 2572, Oct. 2012.
[11] IEC 61008–1, "Type F and type B residual current operated circuit-breakers with and without integral overcurrent protection for household and similar uses," *International standard*, 2009-11.
[12] O. Messal, F. Sixdenier L. Morel and N. Burais, " Thermal behavior of Iron-Nickel-Chromium alloys and correlation with magnetic and physical properties-Part B: Dynamic modeling," *Compumag*, 30 June – 4 July 2013, Budapest, Hungary.
[13] London Metal Exchange, http://www.lme.com.